ADMINISTRATIVE REPORT

AR-384-NASA

May 1968

FINAL REPORT ON SATELLITE METEOROLOGY STUDIES

Administrative Reports of The RAND Corporation are prepared to convey information to its clients on the status of work being done for them. They are not publications intended for distribution to other organizations.

Prepared for: National Aeronautics and Space Administration

Contract No.: NASr-21(07)

The RAND Corporation
1700 MAIN ST. • SANTA MONICA • CALIFORNIA • 90406

INTRODUCTION

RAND work under Contract NASr-21(07) has consisted of basic studies relating to the scientific utilization of meteorological data that may be obtained from unmanned or manned satellites, and to the implications of new satellite techniques and measurements for the development of the science of meteorology.

Principal investigators for this contract were:

Y. H. Katz, June 1963-December 1965

R. E. Huschke, January 1966-April 1968

This Final Report consists of three parts. Part I is a general summary of all research conducted under this contract during the period 1 February 1965 through 31 January 1967. (A summary for the prior period of 12 June 1963 through 31 January 1965 was included in AR-166-NASA, January 1965, and will not be repeated here.) Part II is a detailed discussion of research conducted since 1 February 1967. Part III is a summary of reports issued and personnel active since 1 February 1965.

CONTENTS

PART I: SUMMARY OF RESEARCH
1 February 1965 - 31 January 1967

This two-year period saw the completion of five separate research projects on various aspects of satellites related to atmospheric science, and the beginning of a sixth study which was continued to contract termination. Full titles of cited reports are listed in Part III.

SPHERICS DETECTION FROM SATELLITES

This project had previously established the theoretical feasibility of observing thunderstorm spherics with an isotropic satellite antenna, utilizing the properties of the ionosphere to limit an antenna's field of view. Two questions which arose from this concept were investigated: (1) What amount of directionality could be expected from the ionosphere/antenna system? and (2) What component of the lightning process would radiate the energy receivable by such a system?

It was shown that the field of view could be moderately limited in a reasonably predictable manner if the observed radio frequency lay in the range of 1.3 to 1.5 times the critical frequency of the ionosphere. Below that range the variability of the critical frequency could impose serious errors on estimates of the field of view; above it, the field of view is not appreciably restricted (RM-4949-NASA).

As a step toward answering the second question, an estimate was made of the spectrum radiated by a current streamer whose cross-sectional dimensions are an appreciable fraction of a wavelength and in which the current varies discontinuously with time. Comparison of the theoretical results with experimental measurements suggests that either the radiating streamer has an effective diameter of less than 24 cm (in contrast with visible diameters of one to ten meters), or that the streamer current is not the major source of radiation at frequencies above a few hundred MHz (RM-5242-NASA).

ATMOSPHERIC CIRCULATION ON MARS

Our studies on the atmosphere of Mars centered on the adaptation to Mars of the Mintz-Arakawa general circulation model (a global, two-layer, numerical model of atmospheric circulation). This research was performed in two steps: first, the thermal properties of the Martian surface were investigated, taking into account the presence of an atmosphere, and were incorporated into a method for evaluating heat flow into and out of the atmosphere; second, the numerical experiment was run after the circulation model was modified according to the heating function, atmospheric composition and structure, and astronomical parameters of Mars.

The heating characteristics of the Martian atmosphere were subjected to computer simulation incorporating the effects of radiation, small-scale turbulent convection, and conduction into the ground. The atmosphere was assumed to be CO_2 with a surface pressure of 5 mb. One result was the prediction of a solid CO_2 ice cap with dimensions similar to that of the observed polar cap on Mars (RM-4551-NASA, RM-5017-NASA, P-3262).

The numerical experiment covered 24 Martian days. (The Jet Propulsion Laboratory provided the 7094 computer time.) Important atmospheric features indicated by the experiment were (1) a fluctuating wave regime in the winter hemisphere; (2) a large-amplitude diurnal tide; and (3) condensation of CO_2 to form a winter polar ice cap (RM-5110-NASA).

INVERSE PROBLEMS IN ATMOSPHERIC RADIATIVE TRANSFER

This was a short-lived project (under this contract) specializing in computational approaches to solutions of inverse transfer problems. It extended the previous work of the investigators (on invariant imbedding and perturbation techniques) toward the specific problem of atmospheric radiative transfer (RM-4617-, RM-4637-, RM-4651-, RM-4730-, RM-4775-NASA).

DISTRIBUTION OF CONSTANT-LEVEL BALLOONS

The question of the distribution of a large number of constant-level balloons (used in a global observing system along with satellites and ground stations) was addressed by simulating balloon trajectories using the Mintz-Arakawa general circulation model. In this example, 1000 balloons were followed daily for 45 days of model operation, and their motions were expressed as transition probabilities from one region to another. It was shown how transition probability matrices could be used with real circulation data to develop balloon-launch strategies for an operational system (RM-5018-NASA).

METEOROLOGICAL USEFULNESS OF MANNED SATELLITES

At the special request of the contract monitor, we examined the meteorological usefulness of a manned satellite and proposed a rationale for selecting suitable manned meteorological missions (RM-4462-NASA).

POLAR ENERGY BUDGETS

Based on long-term monthly means (i.e., average annual cycles) a very high correlation was found between Arctic atmospheric heat loss and an atmospheric zonal index one month later (RM-5234-NASA). The substantiation of a physical and predictive relationship would have an important influence on the satellite acquisition of radiation data over polar regions. Several further research steps were indicated, the first of which was to examine the correlation of anomalies of heat loss and circulation over a long time-series of observations. This last investigation was begun at the end of the time period summarized here (January, 1967), and is discussed in detail in Part II.

PART II: REPORT ON POLAR ENERGY BUDGET RESEARCH
1 February 1967 - 30 April 1968

INTRODUCTION

In an earlier phase of this project, we correlated the annual cycles of radiative heat loss from the Arctic atmosphere with a zonal circulation index, using long-term monthly averages of the variables. With the zonal index cycle lagged one month behind the heat-loss cycle, the correlation coefficient was +0.95, compared with coefficients near +0.75 having lags of zero and two months. Two such cycles could easily be astronomically related without being atmospherically so. Nevertheless, some qualitative reasoning regarding the statistical relationship could give credence to a hypothesis that variations in the Arctic atmospheric radiative heat loss cause a predictable delayed response in the strength of the zonal circulation. If this could be shown to be true, a significant increment would be added to the value and urgency of satellite radiation measurements.

We decided to test this hypothesis using long time-series of both the heat loss and a zonal index. In the absence of satellite measurements, the former could be constructed only by radiative flux calculations using radiosonde observations; the latter from a historical series of numerical 500-mb map analyses for the northern hemisphere. The correlation should be made between the anomalies of heat loss and zonal index, in order to eliminate the overbearing influence of the average annual cycle.

One assumption implied by this basic thesis is that the variations in heat content of the Arctic atmosphere are so much larger than those of the tropical atmosphere that the latter can be ignored. It is not clear that this assumption is valid when one is dealing with deviations of heat loss from an average annual cycle. This is a major question to be checked whenever sufficient satellite radiation data have been accumulated.

PROCEDURES

If the advective transport of heat is neglected, atmospheric heat loss, L, can be represented by

$$L = I_\infty - q_a - I_G - F_{s\ell} \qquad (1)$$

where I_∞ is the outgoing longwave radiation from the top of the atmosphere, q_a the shortwave (solar) radiation absorbed by the atmosphere, I_G the net upward longwave radiation at the earth's surface, and $F_{s\ell}$ the net upward latent and sensible heat at the surface.

Given an adequate description of the vertical structure of the atmosphere (in terms of temperature, water vapor, clouds, CO_2, and ozone, each expressed as a function of pressure) the longwave terms of the above expression (I_∞ and I_G) can be theoretically calculated with reasonable confidence, and the shortwave absorption (q_a) with somewhat less confidence. Both radiosonde data and cloud observations are needed, the latter necessitated by the sensitivity of the longwave flux to variations in cloudiness.

The cloud data used in this study were taken from the results of another RAND investigation (as yet unpublished) of the statistical time and space distribution of Arctic cloudiness as derived from surface synoptic observations. Each observation is expressed as one of 16 "cloud distribution models," each model being a different combination of low, middle, and high cloudiness.

For the time period considered in this study, January 1955 through March 1960, all radiosonde data available on magnetic tape for the ring of Arctic land stations shown in Fig. 1 were obtained from the National Weather Records Center. We used only those dates, times, and stations for which there existed matching upper air and cloud data. (The Alaskan stations, Pt. Barrow and Barter Island, had to be omitted completely because no U.S. surface synoptic data are available on magnetic tape at the NWRC, and, therefore, no cloud distributions had been calculated for these two stations. Moreover, we could use no data from the drifting ice stations because the way they are archived makes it impossible to put together matched pairs of surface and radiosonde observations.)

The radiation flux terms were calculated as a smoothed time series of 30-day means computed at 5-day intervals. This was done by first

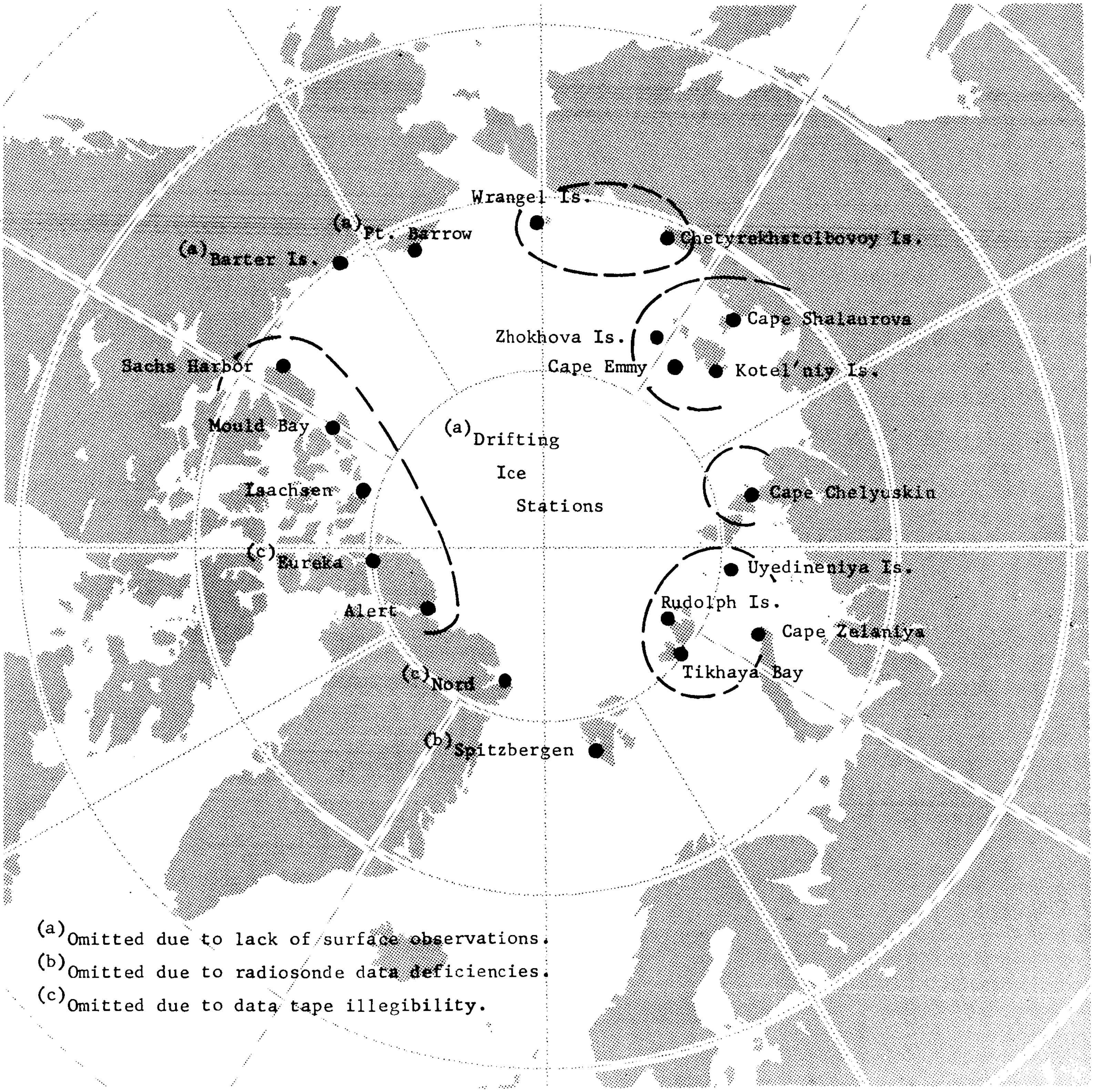

Fig. 1 -- Stations intended for use in radiation calculations.

grouping the stations (as shown in Fig. 1) and considering all soundings of a group to be jointly representative of that region. Thirty-day average soundings were then compiled for each "cloud model," and the radiation terms were calculated for each average sounding. A weighted average of these comprised the final 30-day mean radiative fluxes ($\overline{I}_\infty$, $\overline{I}_G$, and $\overline{q}_a$) for each station group.

For computational efficiency, it was necessary to put all the upper-air soundings into a standard and consistent form. We elected to represent the sounding at 17 pressure levels from the surface to 50 millibars, 9 of which are "mandatory" (standard) levels common to all stations throughout the period being studied.

Both the temperature and relative humidity at intermediate levels were interpolated logarithmically, i.e.:

$$X_j = \frac{X_{j-1}\ \ln\left(\frac{P_{j+1}}{P_j}\right) + X_{j+1}\ \ln\left(\frac{P_j}{P_{j-1}}\right)}{\ln\left(\frac{P_{j+1}}{P_{j-1}}\right)} \tag{2}$$

where X stands for temperature or relative humidity, P is pressure, and j indicates pressure level number, starting at the top of the sounding. When both temperature and height data were available at consecutive standard levels, which was usually the case, the intermediate-level temperature θ_j was evaluated according to

$$\theta_j = \frac{\frac{2g}{R}\left(Z_{j-1} - Z_{j+1}\right) - \left[\theta_{j-1}\ \ln\left(\frac{P_j}{P_{j-1}}\right) + \theta_{j+1}\ \ln\left(\frac{P_{j+1}}{P_j}\right)\right]}{\ln\left(\frac{P_{j+1}}{P_{j-1}}\right)} \tag{3}$$

where Z is height, g the acceleration of gravity, R the gas constant, and the units are meters, seconds, and degrees Kelvin. This expression will reproduce with reasonable fidelity (for our purposes), for example, a strong temperature inversion between the surface and 850 mb.

All soundings that did not extend to at least 300 mb were discarded. Essentially all others were used, even if humidities were missing, as was often the case. Where necessary, missing temperatures above 300 mb were inserted by applying the climatological average lapse rate (for that month and latitude) between 300 mb and 200 mb and assuming the temperatures constant from 200 mb upward. Missing humidities were inserted by using averages calculated for the same region, season, and cloud distribution.

Thus we produced a complete set of individual "reconstituted" soundings. To calculate the radiation terms using individual soundings is desirable, but the computer time necessary is exorbitant. Therefore, the previously mentioned 30-day average soundings were calculated. It should be noted that temperatures were averaged as the fourth root of the sum of temperatures to the fourth power, in order to approximate the proper weighting for the radiation calculations.

The method and spectral data of Rodgers and Walshaw (1966) were used to calculate the longwave terms, I_∞ and I_G. They can be expressed in the forms

$$I_\infty = \sum_{i=1}^{N} \left\{ T_i(\phi_T, \phi_n) \left[B_i(\theta_G) - B_i(\theta_n) \right] \left[1 - f(\phi_n) \right] + B_i(\theta_T) - \int_{B_i(\theta_n)}^{B_i(\theta_T)} \left[1 - f(\phi) \right] \cdot T_i(\phi_T, \phi)\, dB_i(\theta) \right\} , \tag{4}$$

and

$$I_G = \sum_{i=1}^{N} \left\{ \left[B_i(\theta_G) - B_i(\theta_n) \right] + \left[1 - f^*(\phi_T) \right] \cdot T_i(\phi_T, \phi_n) \cdot B_i(\theta_T) - \int_{B_i(\theta_n)}^{B_i(\theta_T)} \left[1 - f^*(\phi) \right] \cdot T_i(\phi, \phi_n)\, dB_i(\theta) \right\} . \tag{5}$$

In these expressions, $B_i\,[\theta(\phi)]$ is the Planck function in the ith spectral interval corresponding to the temperature θ at the atmospheric level $\phi = P/P_o$, where P is pressure and $P_o \equiv 1000$ millibars. $T_i(\phi_T,\phi)$ is the transmission function in the ith spectral interval between level ϕ and the uppermost computation level $\phi_T = .05$ ($P_T = 50$ mb); $T_i(\phi,\phi_n)$ is the corresponding transmission function between ϕ and the surface, for which $\phi = \phi_n$. In these formulas we distinguish between the ground temperature θ_G and the surface air temperature θ_n, but in carrying out the actual calculations it was assumed that these temperatures are identical, and the terms involving $B_i(\theta_G) - B_i(\theta_n)$ thus vanish. The quantities $f(\phi)$ and $f^*(\phi)$ incorporate the effects of cloudiness, being that fraction of the field of view obscured at and beyond the level ϕ by clouds between the observer and level ϕ; $f(\phi)$ is for an observer looking down into the atmosphere, $f^*(\phi)$ for an observer looking up from the ground. This simple incorporation of cloud effects in the model is based on the assumptions (a) that all clouds are black in the infrared, and (b) that the fractional coverages, f and f^*, are characteristic not only of the whole sky, but also of each angle of view downward or upward in the atmosphere.

The transmission functions were evaluated using the Rodgers and Walshaw expressions (6) through (9), and spectral data were taken from their Tables 3, 5, and 6 for the rotation band and 6.3-micron band of water vapor, and for the 15-micron band of CO_2. The angular integration was accomplished simply by using the flux diffusivity factor $\delta = 1.66$. Certain spectral regions require special treatment. The wave-number region from 585 to 755 cm^{-1} includes the 15-micron band, and here the effective transmission function was taken to be the product of the individual transmission functions for CO_2 and H_2O. The region from 800 to 1000 cm^{-1} corresponds to the water-vapor continuum, and for this region the transmission function was taken to be

$$T(\phi_j,\phi_k) = \exp(-0.1\,\bar{m}\delta) \qquad (6)$$

(see Goody, 1964, p. 195), where $\bar{m}(\phi_j,\phi_k)$, in gm/cm^2, is the Curtis-Godson mean path length between levels ϕ_j and ϕ_k (see formula (7) of

Rodgers and Walshaw). The regions from 900 to 1000 cm^{-1} and from 2200 to 2800 cm^{-1} correspond to ozone bands. Rather than attempt a detailed incorporation of ozone effects, we rather arbitrarily assumed that 80 percent of the radiation in these bands comes from the stratosphere having the temperature $\theta(\phi_T)$ at the top of the sounding, with the remaining 20 percent coming from cloud tops and ground for I_∞, or from space ($\theta = 0$) for I_G.

Several tests of integration procedures showed that for temperature and humidity distributions varying linearly between our selected pressure levels, simple quadrilateral evaluation of the integrals over ϕ gives accuracies within 2 percent for I_∞ and I_G; this integration method was used.

Solar radiation absorbed in the atmosphere, q_a, was calculated by a method suggested by Hanson, Vonder Haar, and Suomi (1967) on the basis of empirical studies of the gross energy balance over North America. Following this method we write

$$q_a = \frac{1}{t_m} \int_0^{t_m} S_o \sin\alpha \cdot \left\{ 0.096 + 0.045 \left[\left(\frac{u}{\sin\alpha} \right)^{1/2} \ln \left(\frac{u}{\sin\alpha} \right) \right] \right\} , \tag{7}$$

where t_m is the 30-day averaging period, S_o the solar constant, $\alpha(t)$ the solar elevation angle, and u the total precipitable water content of the atmosphere, evaluated from our data as

$$u = \frac{P_o}{2g} \sum_{j=1}^{n-1} \left(\mu_j + \mu_{j+1} \right) \left(\phi_{j+1} - \phi_j \right) . \tag{8}$$

In this expression, μ_j is the specific humidity at level ϕ_j. The integrand of the equation for q_a must be taken to be zero for nighttime hours ($\sin\alpha \le 0$). Rather than calculating that integral, in view of the other uncertainties of the problem, we approximate it by

$$q_a \cong \frac{t^*}{t_m} S_o \overline{\sin\alpha} \left\{0.096 + 0.045 \left[\left(\frac{u}{\sin\alpha}\right)^{1/2} \ell n \left(\frac{u}{\sin\alpha}\right)\right]\right\}, \tag{9}$$

where t^*/t_m is the 30-day average daily fraction of the daylight part of the day, and $\overline{\sin\alpha}$ is the corresponding average elevation angle for the daylight part of the day.

In comparison with the other three terms in our expression for the atmospheric heat loss, the sensible and latent heat flux at the surface, $F_{s\ell}$ is small and exhibits little year-to-year variability. We have chosen to represent it as a single average annual cycle based on values given by Doronin (1966, p. 252). Our values are the sum of Doronin's values for eddy heat exchange and heat loss by evaporation in the Central Arctic. Values for all of the overlapping 30-day averaging periods in the year were obtained by graphical interpolation.

For correlation with the radiation parameters, three series of zonal circulation indices were calculated from 500-mb northern hemisphere grid-point data furnished to us by the National Center for Atmospheric Research. The three types of index are a North Atlantic index (Z_{atl}), a North Pacific index (Z_{pac}), and a circumglobal index (Z_{belt}). All three consist of the average difference between the height of the 500-mb surface at two latitudes: Z_{atl} at latitudes 60^oN and 70^oN in the sector from 40^oW to 30^oE; Z_{pac} at latitudes 50^oN and 60^oN in the sector from 170^oE to 120^oW; and Z_{belt} at the latitudes 60^oN and 70^oN completely around the globe (see Fig. 2). As a rough measure of the meridionality of the circulation, we also computed the standard deviations (σ) of 500-mb heights around the 50, 60, and 70^oN latitude circles. Finally, "unfiltered" wave numbers (K) were calculated around the same three latitudes simply by taking one-half the number of times the mean height contour crossed the latitude circle. Thirty-day mean values of all these nine circulation parameters were calculated to correspond in time exactly with the radiation parameters.

As the next-to-last step in preparing the time series for lag correlations, the atmospheric heat loss terms, L, that had been individually calculated for each group of stations (as shown in Fig. 1), were

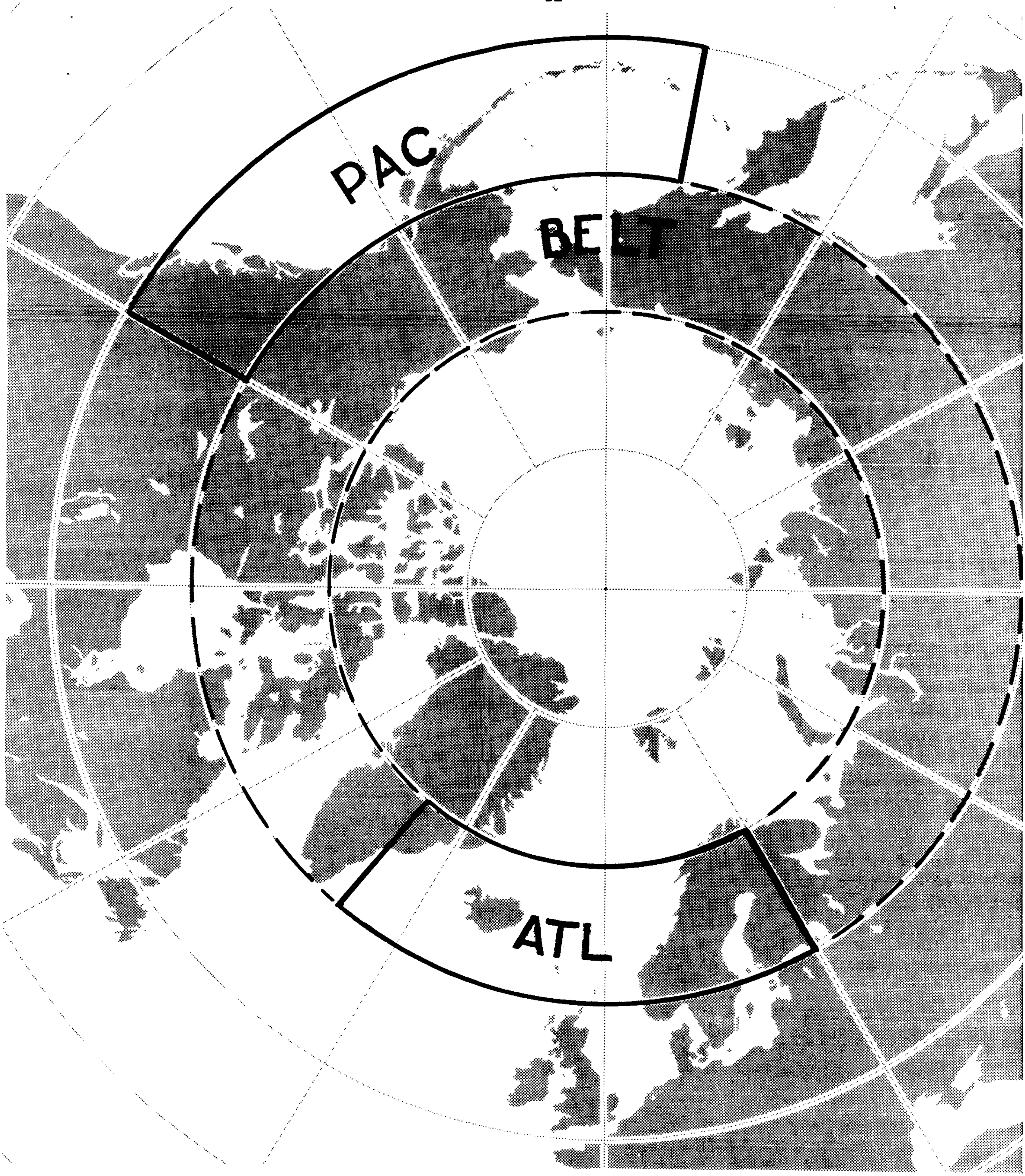

Fig. 2 -- Areas represented by the three zonal circulation indices: Z_{atl}, Z_{pac}, Z_{belt}.

spatially averaged into a single time series purporting to represent the entire Arctic. The drop-out, along the way, of five land stations and all the drifting ice stations undoubtedly compromised the representativeness of this average heat loss figure, $\bar{L}$; how seriously, we cannot tell. The most serious deficiency was probably the lack of usable data from the ice stations of the Central Arctic.

The final step was to subtract out the average annual cycles from the time series of all the variables to be correlated. Thus, an individual value in the resulting time series is represented by the deviation of its original value from its 5-year mean value for the same 30-day calendar period.

One weakness in this latter procedure is that five years is not long enough to establish a reliable and smooth average annual cycle. In fact, the curves of the average annual cycles were quite irregular, and the deviations from these curves were therefore less meaningful than if long-period averages had been available and used.

Another unanticipated deficiency in our method arose in the calculation of the atmospheric absorption term, q_a. Here, the only independent variables were the water-vapor content of the atmosphere and the astronomical terms. The resulting values of q_a were smaller by a factor of 3 or 4 than those assumed by most Arctic researchers; and, more important in this study, they showed so little year-to-year variation that their contribution to the deviation series of L was essentially nil. Actually, of course, the cloudiness and high surface albedo of the Arctic, together with the low sun angle, could combine to increase greatly the amount of shortwave radiation absorbed by the atmosphere. The expression that we used (see p. 11) was derived from satellite measurements over the United States, and implicitly took into account cloud conditions. However, the low water-vapor contents that imply clear skies in middle latitudes are often associated with extensive cloudiness in the Arctic. Therefore, our failure to account explicitly for the effects of Arctic clouds and albedo was tantamount to neglecting q_a altogether. Since the latent and sensible heat flux at the surface, $F_{s\ell}$, was <u>given</u> as an annual cycle,

$$\overline{L}' \cong (\overline{I_{\infty} - I_G})' , \qquad (10)$$

where the primes indicate deviations from a 5-year average annual cycle.

RESULTS

We computed multilag correlation coefficients between $\overline{L}'$ (the deviation from average atmospheric heat loss) and all nine deviation series of circulation parameters. The lags ranged from -3 months (meaning $\overline{L}'$ now and the circulation parameter 3 months earlier) to +5 months (meaning $\overline{L}'$ now and the circulation parameter 5 months later). These coefficients are plotted in Figs. 3, 4, and 5. The significance levels shown were derived by testing the null hypothesis that the series were not correlated. Thus, there is a chance of only one in a thousand that a correlation coefficient of magnitude > .175 is not "real."

Although none of the correlation coefficients is very large in an absolute sense, which is certainly not surprising, some interestingly "significant" correlations do appear. At this point we cannot discuss any cause-and-effect implications, but simply call attention to certain features of the results.

The most interesting set of correlations is found with circulation parameters lagged 2½ months behind the heat loss. Note that on Figs. 3 and 5, Z'_{atl}, Z'_{belt}, and K'_{70} all show significant maximum positive correlations, and K'_{50} shows a very significant maximum negative correlation at this lag of 2½ months. The corresponding correlations with σ' (Fig. 4) are all notably low and insignificant. This could indicate a tendency, 2½ months after a period of anomalously high atmospheric heat loss in the Arctic, for cyclones to be displaced anomalously poleward, accompanied by a corresponding strong zonal circulation immediately south of the cyclones.

We had really expected to see the most significant correlations when the circulation was lagged about one month behind the heat loss, for the superficial reason that the correlation between annual cycles was highest with this lag (see p. 4). In this analysis using deviations, σ'_{60} and σ'_{70} show significant maxima of positive correlation at a lag of

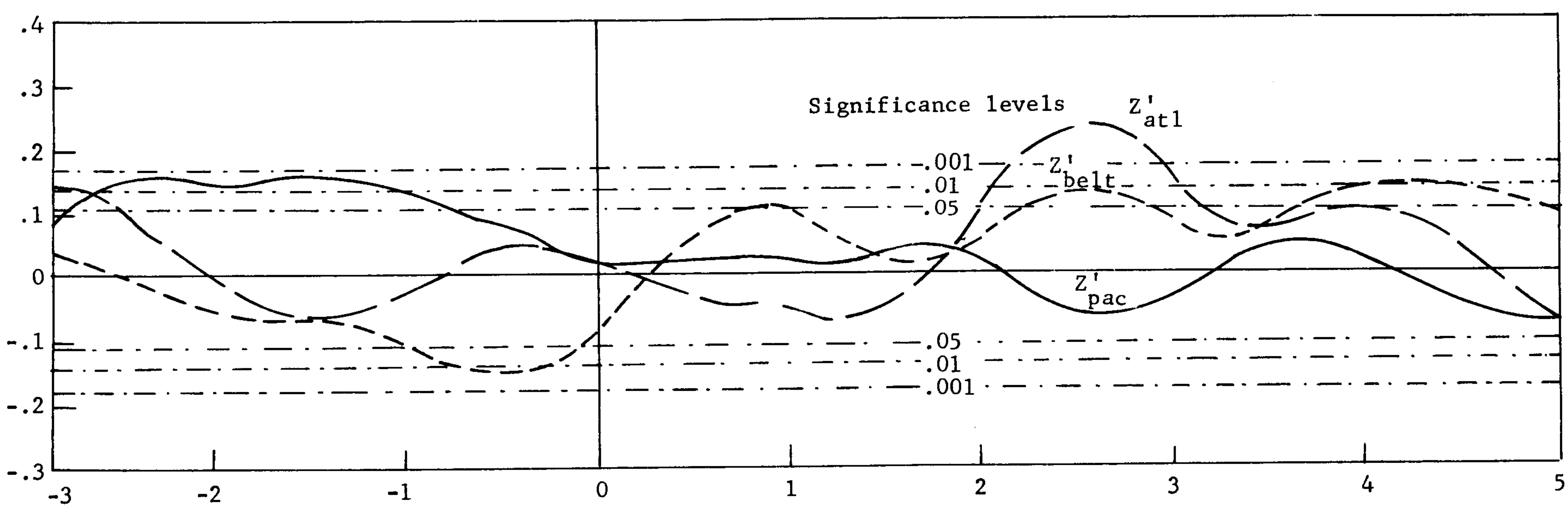

Fig. 3 -- Lag correlations of the deviations of Arctic atmospheric heat loss, $\overline{L}'$, vs. the deviations of zonal circulation indices, Z'_{atl}, Z'_{pac}, Z'_{belt}.

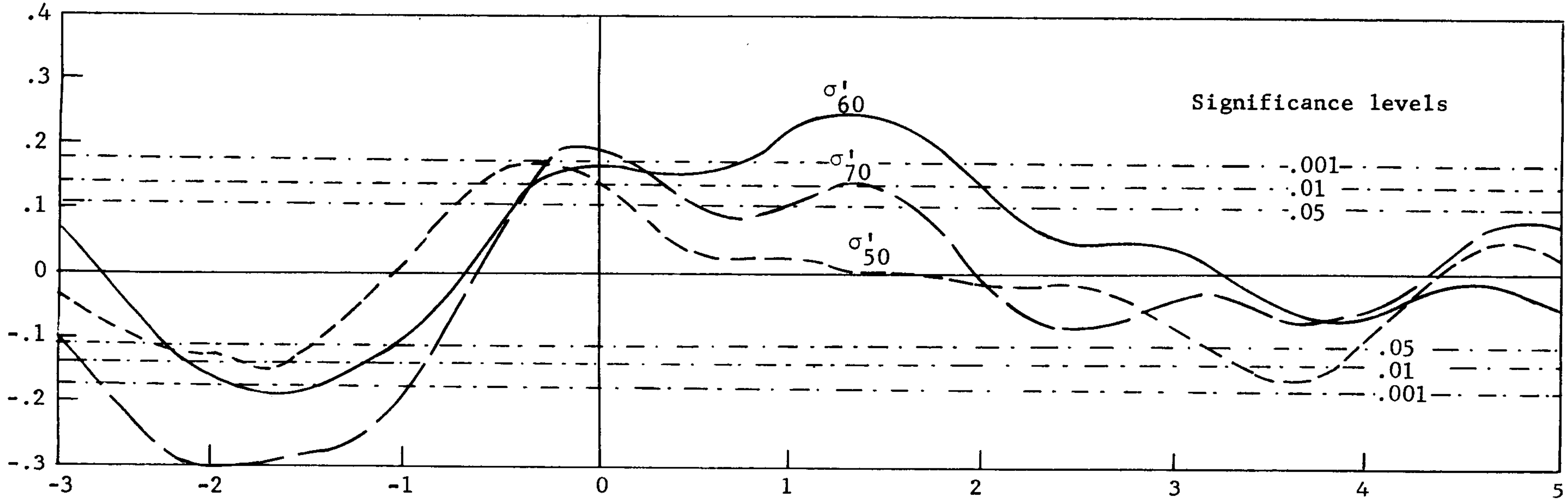

Fig. 4 -- Lag correlations of the deviations of Arctic atmospheric heat loss, $\overline{L}'$, vs. the deviations of the standard deviations of 500-mb height, σ'_{50}, σ'_{60}, σ'_{70}.

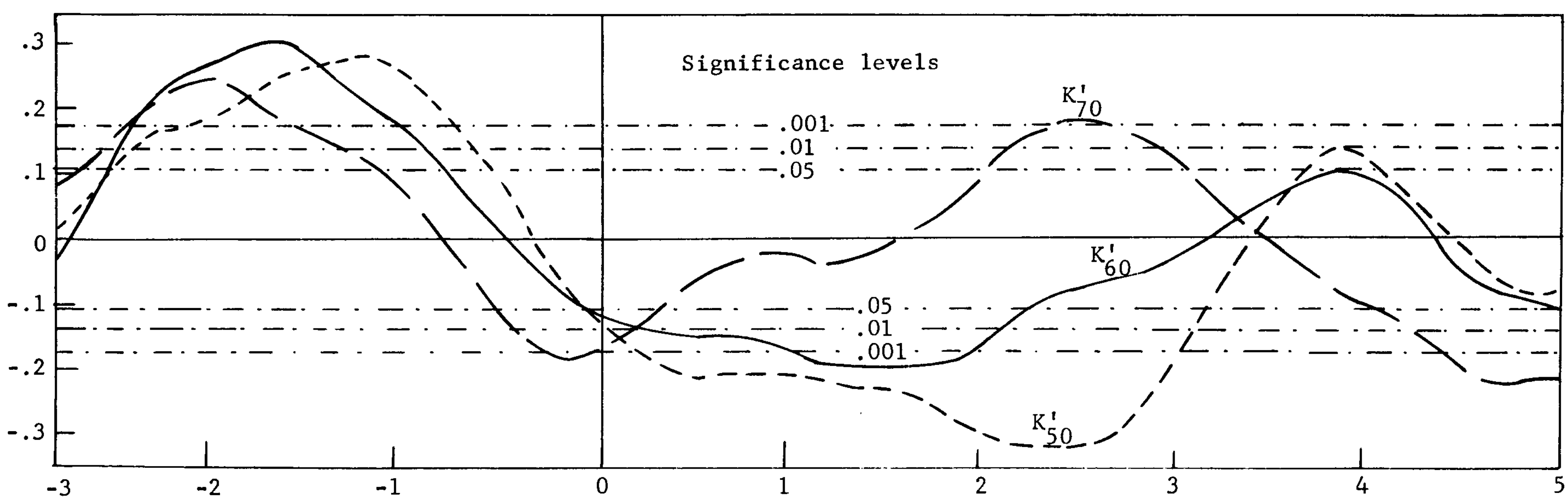

Fig. 5 -- Lag correlations of the deviations of Arctic atmospheric heat loss, $\overline{L}'$, vs. the deviations of unfiltered hemispheric wave numbers, K'_{50}, K'_{60}, K'_{70}.

slightly more than one month, and the wave-number deviation K'_{50} and K'_{60} show significant negative correlations. This could indicate a tendency toward strong meridionality about a month after anomalously high heat loss from the polar atmosphere, or conversely, a tendency toward a weak, confused, subarctic circulation following low heat loss.

One of the striking implications of this analysis lies in the fairly strong and very significant correlations (with heat loss) of the standard deviation and wave number anomalies at lags of -1 to -2 months. The indication is that the meridionality of the circulation affects the Arctic heat balance 1 to 2 months later in some predictable way.

GENERAL DISCUSSION

The atmosphere works to maintain a global thermodynamic balance. The principal "thermal forcing function" on atmospheric circulation is the thermal gradient from equator to pole, which exhibits not only an annual cycle but significant fluctuations about that cycle. Presumably, the atmosphere responds in some deterministic way to all variations in the meridional thermal gradient; its response will, in turn, affect the thermal gradient; and so on. This familiar concept has never been directly applied to practical prediction problems, mainly because the necessary radiative transfer calculations have been too complex and uncertain to perform with surface-based observations. Radiation measurements by satellite open the door to this application.

What we have done is try to anticipate the advent of regular satellite measurements by simulating one kind of radiation parameter that satellites could make available on a practical basis, and using this inferior simulation, to explore a possible relationship between radiation and circulation.

The results do not lead immediately to a new and clear long-range weather prediction technique--they could not be expected to, for many reasons. But, the correlations found here do sustain our optimism that predictable time-delayed interactions will be found between major radiation and circulation parameters, once good data are available and better physical models are applied.

PART III: PUBLISHED REPORTS AND ACTIVE PERSONNEL

TECHNICAL REPORTS

1. RM-4462-NASA, Some Comments on the Meteorological Usefulness of a Manned Satellite, S. M. Greenfield, M. H. Davis, D. Deirmendjian, Y. H. Katz, C. B. Leovy, and R. R. Rapp, February 1965.
2. RM-4551-NASA, Note on Thermal Properties of Mars, C. B. Leovy, April 1965.
3. RM-4617-NASA, Numerical Estimation of Derivatives with an Application to Radiative Transfer in Spherical Shells, H. H. Kagiwada, R. E. Kalaba, and R. E. Bellman, June 1965.
4. RM-4637-NASA, Estimation of Internal Source Distributions Using External Field Measurements in Radiative Transfer, R. E. Bellman, H. H. Kagiwada, and R. E. Kalaba, June 1965.
5. RM-4651-NASA, The Invariant Imbedding Equation for the Dissipation Function of a Homogeneous Finite Slab, R. E. Bellman, H. H. Kagiwada, R. E. Kalaba, and S. Ueno, July 1965.
6. RM-4730-NASA, Invariant Imbedding and Perturbation Techniques Applied to Diffuse Reflection from Spherical Shells, R. E. Bellman, H. H. Kagiwada, R. E. Kalaba, August 1965.
7. RM-4775-NASA, Computational Results for Diffuse Transmission and Reflection for Homogeneous Finite Slabs with Isotropic Scattering, R. E. Kalaba, R. E. Bellman, H. H. Kagiwada, and S. Ueno, October 1965.
8. RM-4949-NASA, The Effective Directivity of an Isotropic Antenna Looking Down Through the Ionosphere, R. L. Kirkwood, June 1966.
9. RM-5017-NASA, Radiative-Convective Equilibrium Calculations for a Two-Layer Mars Atmosphere, C. B. Leovy, May 1966.
10. RM-5018-NASA, Probabilistic Dynamics of a Global Horizontal Sounding System, R. R. Rapp, May 1966.
11. RM-5110-NASA, A Numerical General Circulation Experiment for the Atmosphere of Mars, C. B. Leovy and Y. Mintz, December 1966.
12. RM-5234-NASA, An Apparent Statistical Relationship Between Polar Heat Budget and Zonal Circulation, R. R. Rapp, J. O. Fletcher, and R. E. Huschke, January 1967.

13. P-3262, Some Aspects of the Circulation of Mars, C. B. Leovy, November 1965, for the Proceedings of the Conference on Exploration of the Planets, Virginia Polytechnic Institute (Blacksburg, Virginia, August 1965).

14. RM-5242-NASA, The Relation Between the Diameter of a Lightning Streamer and its Radiated Radio Frequency Spectrum, R. L. Kirkwood, January 1967.

ADMINISTRATIVE REPORTS

The following administrative reports were forwarded to NASA Headquarters:

1. AR-188-NASA, Status Report on Satellite Meteorology Studies, May 1965.
2. AR-201-NASA, Status Report on Satellite Meteorology Studies, August 1965.
3. AR-219-NASA, Status Report on Satellite Meteorology Studies, November 1965.
4. AR-236-NASA, Status Report on Satellite Meteorology Studies, February 1966.
5. AR-255-NASA, Status Report on Satellite Meteorology Studies, May 1966.
6. AR-273-NASA, Status Report on Satellite Meteorology Studies, August 1966.
7. AR-289-NASA, Status Report on Satellite Meteorology Studies, November 1966.
8. AR-304-NASA, Status Report on Satellite Meteorology Studies, February 1967.
9. AR-315-NASA, Status Report on Satellite Meteorology Studies, May 1967.
10. AR-333-NASA, Status Report on Satellite Meteorology Studies, August 1967.
11. AR-348-NASA, Status Report on Satellite Meteorology Studies, November 1967.
12. AR-367-NASA, Status Report on Satellite Meteorology Studies, February 1968.

SCIENTIFIC PERSONNEL ACTIVE DURING THE CONTRACT PERIOD

R. E. Bellman, K.J.K. Buettner (Consultant), M. A. Carter, M. H. Davis, D. Deirmendjian, J. O. Fletcher, S. M. Greenfield, R. E. Huschke, H. H. Kagiwada, R. E. Kalaba, Y. H. Katz, R. L. Kirkwood, C. B. Leovy, A. H. Marcus (Consultant), Y. Mintz (Consultant), A. B. Nelson, S. M. Olenicoff, R. R. Rapp, E. E. Rodriguez, Z. Sekera (Consultant).

REFERENCES

Goody, R. M., Atmospheric Radiation, Oxford University Press, 1964.

Hanson, K. J., T. H. Vonder Haar, and V. E. Suomi, "Reflection of Sunlight to Space and Absorption by the Earth and Atmosphere over the United States During Spring 1962," Monthly Weather Review, Vol. 95, No. 6, June 1967.

Huschke, R. E., J. O. Fletcher, and R. R. Rapp, An Apparent Statistical Relationship Between Polar Heat Budget and Zonal Circulation, RM-5234-NASA, The RAND Corporation, Santa Monica, California, January 1967.

Rodgers, C. D., and C. D. Walshaw, "The Computation of Infrared Cooling in Planetary Atmospheres," Quart. J. Roy. Met. Soc., Vol. 92, p. 67, 1966.